

Monoacylglycerol lipase reprograms hepatocytes and macrophages to promote liver regeneration

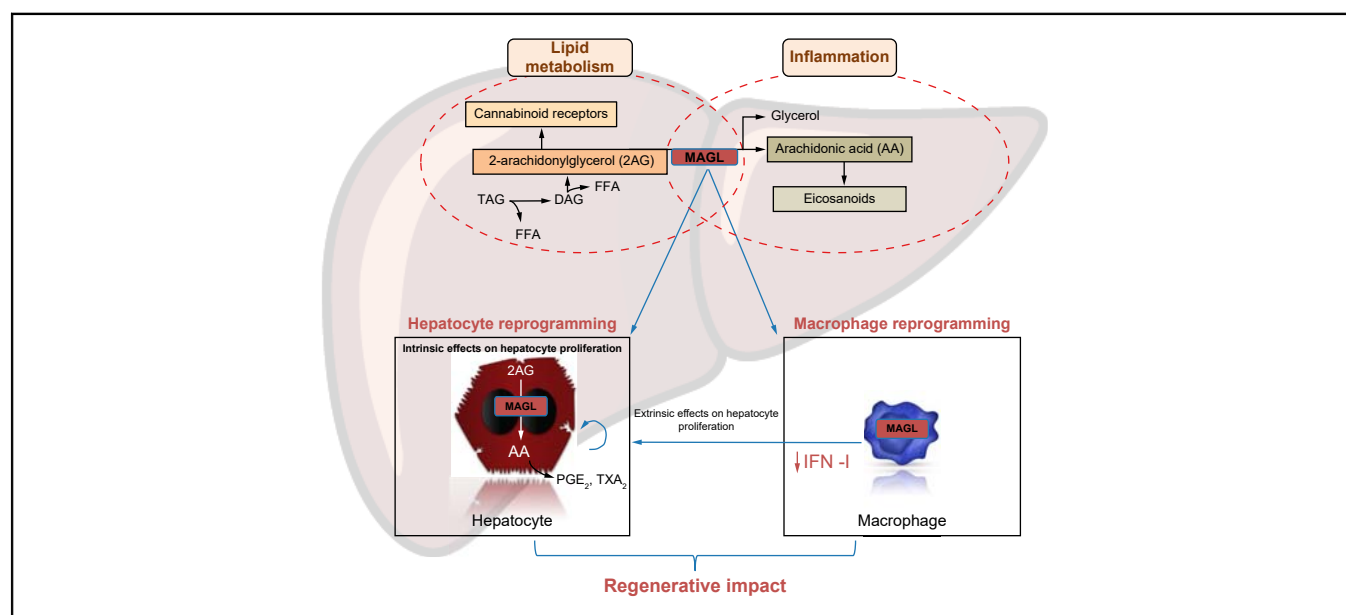
Authors

Manon Allaire, Rola Al Sayegh, Morgane Mabire, Adel Hammoutene, Matthieu Siebert, Charles Caër, Mathilde Cadoux, JingHong Wan, Aida Habib, Maude Le Gall, Pierre de la Grange, Hervé Guillou, Catherine Postic, Valérie Paradis, Sophie Lotersztajn, H el ene Gilgenkrantz

Correspondence

helene.gilgenkrantz@inserm.fr (H. Gilgenkrantz).

Graphical abstract



Highlights

- Monoacylglycerol lipase (MAGL) reduces hepatocyte proliferation in human precision-cut liver slices.
- Inhibiting MAGL specifically in hepatocytes delays liver regeneration by reducing liver 2-arachidonylglycerol production.
- Inhibiting MAGL specifically in myeloid cells delays liver regeneration by reprogramming macrophages towards the IFN-1 pathway.
- Neutralising the IFN-1 pathway restores liver regeneration in mice invalidated for MAGL in myeloid cells.

Impact and Implications

By using human liver samples and mouse models of global or specific cell type invalidation, we show that the monoacylglycerol pathway plays an essential role in liver regeneration. We unveil the mechanisms by which MAGL expressed in both hepatocytes and macrophages impacts the liver regeneration process, via eicosanoid production by hepatocytes and the modulation of the macrophage interferon pathway profile that restrains hepatocyte proliferation.



Monoacylglycerol lipase reprograms hepatocytes and macrophages to promote liver regeneration

Manon Allaire,^{1,2} Rola Al Sayegh,¹ Morgane Mabire,¹ Adel Hammoutene,^{1,3} Matthieu Siebert,^{1,4} Charles Caër,¹ Mathilde Cadoux,¹ JingHong Wan,¹ Aida Habib,⁵ Maude Le Gall,¹ Pierre de la Grange,⁶ Hervé Guillou,⁷ Catherine Postic,⁸ Valérie Paradis,^{1,3} Sophie Lotersztajn,¹ Hélène Gilgenkrantz^{1,*}

¹Université de Paris, INSERM, U1149, CNRS, ERL 8252, Centre de Recherche sur l'Inflammation (CRI), Laboratoire d'Excellence Inflammex, Paris, France; ²AP-HP Sorbonne Université, Hôpital Universitaire Pitié Salpêtrière, Service d'Hépatogastroentérologie, Paris, France; ³Department of Pathology, Assistance Publique-Hôpitaux de Paris and Université de Paris, Hôpital Beaujon, Clichy, France; ⁴Surgery Department, Hôpital Bichat-Claude Bernard, APHP, Université de Paris, Paris, France; ⁵Department of Basic Medical Sciences, College of Medicine, QU Health Qatar University, Doha, Qatar; ⁶GenoSplice, Paris, France; ⁷Toxalim (Research Centre in Food Toxicology), INRAE, ENVT, INP-Purpan, PS, Université de Toulouse, Toulouse, France; ⁸Université de Paris, Institut Cochin, INSERM U1016, CNRS, Paris, France

JHEP Reports 2023. <https://doi.org/10.1016/j.jhepr.2023.100794>

Background & Aims: Liver regeneration is a repair process in which metabolic reprogramming of parenchymal and inflammatory cells plays a major role. Monoacylglycerol lipase (MAGL) is an ubiquitous enzyme at the crossroad between lipid metabolism and inflammation. It converts monoacylglycerols into free fatty acids and metabolises 2-arachidonoylglycerol into arachidonic acid, being thus the major source of pro-inflammatory prostaglandins in the liver. In this study, we investigated the role of MAGL in liver regeneration.

Methods: Hepatocyte proliferation was studied *in vitro* in hepatoma cell lines and *ex vivo* in precision-cut human liver slices. Liver regeneration was investigated in mice treated with a pharmacological MAGL inhibitor, MJN110, as well as in animals globally invalidated for MAGL (MAGL^{-/-}) and specifically invalidated in hepatocytes (MAGL^{Hep^{-/-}}) or myeloid cells (MAGL^{Mye^{-/-}}). Two models of liver regeneration were used: acute toxic carbon tetrachloride injection and two-thirds partial hepatectomy. MAGL^{Mye^{-/-}} liver macrophages profiling was analysed by RNA sequencing. A rescue experiment was performed by *in vivo* administration of interferon receptor antibody in MAGL^{Mye^{-/-}} mice.

Results: Precision-cut human liver slices from patients with chronic liver disease and human hepatocyte cell lines exposed to MJN110 showed reduced hepatocyte proliferation. Mice with global invalidation or mice treated with MJN110 showed blunted liver regeneration. Moreover, mice with specific deletion of MAGL in either hepatocytes or myeloid cells displayed delayed liver regeneration. Mechanistically, MAGL^{Hep^{-/-}} mice showed reduced liver eicosanoid production, in particular prostaglandin E₂ that negatively impacts on hepatocyte proliferation. MAGL inhibition in macrophages resulted in the induction of the type I interferon pathway. Importantly, neutralising the type I interferon pathway restored liver regeneration of MAGL^{Mye^{-/-}} mice.

Conclusions: Our data demonstrate that MAGL promotes liver regeneration by hepatocyte and macrophage reprogramming. **Impact and Implications:** By using human liver samples and mouse models of global or specific cell type invalidation, we show that the monoacylglycerol pathway plays an essential role in liver regeneration. We unveil the mechanisms by which MAGL expressed in both hepatocytes and macrophages impacts the liver regeneration process, via eicosanoid production by hepatocytes and the modulation of the macrophage interferon pathway profile that restrains hepatocyte proliferation.

© 2023 The Author(s). Published by Elsevier B.V. on behalf of European Association for the Study of the Liver (EASL). This is an open access article under the CC BY-NC-ND license (<http://creativecommons.org/licenses/by-nc-nd/4.0/>).

Introduction

Liver regeneration represents a major therapeutic issue following acute liver damage such as large surgical resections, toxic injury, or ischaemia/reperfusion lesions induced by liver transplantation. This wound healing process requires timely coordinated epithelial and immune cell interactions, allowing hepatocytes to quit their quiescent state to proliferate and the

liver to recover rapidly. During regeneration, not only hepatocytes but also immune cells – particularly macrophages – undergo metabolic rewiring.^{1–3} Emerging data suggest that targeting the metabolism of these cells could constitute a new therapeutic strategy to stimulate liver regeneration.^{1–3} However, molecular mediators linking metabolism and liver regeneration remain poorly known.

Monoacylglycerol lipase (MAGL) is a rate-limiting enzyme in the degradation of monoacylglycerols that are hydrolysed into glycerol and free fatty acids. MAGL produces arachidonic acid from 2-arachinoylglycerol and is also the primary source for pro-inflammatory prostaglandins (PGs) in the liver. This makes this ubiquitously expressed protein a connecting hub between lipids

Keywords: Wound healing; Injury; MAGL; Proliferation.

Received 20 October 2022; received in revised form 21 April 2023; accepted 26 April 2023; available online 16 May 2023

* Corresponding author. Address: Université de Paris, INSERM, U1149, CNRS, ERL 8252, Centre de Recherche sur l'Inflammation (CRI), Laboratoire d'Excellence Inflammex, F-75018 Paris, France. Tel.: +33 157277530

E-mail address: helene.gilgenkrantz@inserm.fr (H. Gilgenkrantz).



ELSEVIER



and inflammation.^{4–7} We recently unraveled MAGL as a novel immunometabolic target allowing, when inhibited, to slow down liver fibrosis in the context of chronic liver injury.⁸ However, the role of MAGL in the liver regeneration context had never been investigated. We thus wondered to what extent MAGL, and particularly MAGL expressed by macrophages and hepatocytes, besides its pro-fibrogenic role, might also modulate liver regeneration.

In the present study, we combined experiments in human samples and mice models to study the central role of MAGL in liver regeneration. We demonstrated that in hepatocytes MAGL induces eicosanoids production that promotes their proliferation. Using RNA sequencing (RNASeq), we showed that MAGL deficiency reprograms liver macrophages expression profile and induces type I interferon (IFN-I) pathway. Our results highlight the regenerative properties of MAGL in the liver by both an intrinsic direct lipid reprogramming of hepatocytes and an extrinsic reprogramming of macrophage expression profile.

Materials and methods

Generation of invalidated mice

MAGL-deficient mice (MAGL^{-/-}) were backcrossed for more than 10 generations on a C57BL/6J background. C57BL/6J control mice were purchased from Janvier (Le Genest-Saint-Isle, France). *Mgll-oxP/loxP* mice (MAGL^{fl/fl}) and MAGL-myeloid mice (MAGL^{Mye-/-}) were generated as previously described.⁸ MAGL^{Hep-/-} mice were generated by crossing MAGL^{fl/fl} to *Alb-Cre* (B6.Cg-Speer6-*ps1Tg(Alb-cre)* 21Mgn/J Jackson Laboratory) for more than 10 generations. Animals were housed in a pathogen-free animal facility and fed *ad libitum*.

Human liver samples

Patients

Liver samples were obtained from seven patients with fibrosis (F2 to F4 according to the METAVIR score system; see Table 1) undergoing liver resection or liver transplantation at the digestive surgical department of Beaujon Hospital (Clichy, France). Patients' clinical data are presented in Table 1. All patients gave written consent to participate in this study, which complied with the ethical guidelines of the 1975 Declaration of Helsinki. Fresh liver specimens were examined by a pathologist, and samples were collected at distance from the tumour (when present) and surgical margins.

Human ex vivo PCLS

Fresh liver specimens were harvested and immediately kept on ice in sterile University of Wisconsin solution (Belzer UW[®] Cold Storage Solution, Bridge to Life, BTLBUW-1000). Liver cores were generated from liver specimens using 8-mm-diameter biopsy

punches, embedded into 5% low-gelling-temperature agarose (Sigma Aldrich) and mounted in a tissue slicer (automated vibrating blade microtome, Leica Biosystems VT1200 S) filled with HBSS supplemented with 25 mM of D-Glucose (Sigma Aldrich), 100 µg/ml streptomycin, and 1 µg/ml amphotericin B (Gibco[™]). Precision-cut liver slices (PCLS, 8-mm diameter, 250-µm thickness) were generated using the following slicing parameters: speed, 0.5 mm/s; thickness, 250 µm; and amplitude, 3 mm. Human PCLS were transferred on 8-µm polyethylene terephthalate tissue culture inserts (ThinCert[™], Greiner Bio-One) in six-well plates and pre-incubated in William's E Medium (Gibco[™]) supplemented with 100 IU/ml penicillin and 100 µg/ml streptomycin, 1 µg/ml amphotericin B (Gibco[™]), and 25 mM D-Glucose (Sigma Aldrich). After 1-h pre-incubation, fresh culture medium containing 10 µM MJN110 or its vehicle (0.01% DMSO) was added, and PCLS were cultivated at 37 °C, 5% CO₂, under a continuous gentle orbital agitation during 2 days. Culture medium was renewed daily. After 48 h of culture, PCLS were washed in cold PBS and fixed in 10% formalin for 24 h for immunohistochemistry experiments.

Experimental mouse models of liver regeneration

Partial hepatectomy

Ten- to 16-week-old male mice were submitted to two-thirds partial hepatectomy (PHx) as previously described.⁹ Animals were sacrificed 40 h, 48 h, or 14 days after PHx.

CCl₄-induced injury and in vivo injections

Ten- to 16-week-old male mice received one intraperitoneally (i.p.) injection (0.6 ml/kg body weight [BW]) of carbon tetrachloride (CCl₄) (Sigma-Aldrich 87030) diluted 1/10 in mineral oil (Sigma-Aldrich M-5310). Control animals received mineral oil. When indicated, mice were i.p. injected with the MAGL inhibitor MJN110 (Cayman Chemical 17583), or its vehicle (Emulphor: ethanol:PBS 1:1:18, 10 mg/kg BW), 2 h before CCl₄ injection and then daily until sacrifice. When indicated, anti-mouse interferon α/β receptor (IFNAR) 1 antibody (Bio Cell BE0241), or its isotype (Bio Cell BE0083), was injected i.p. the day before CCl₄ injection (500 µg), 1 h before CCl₄ injection (450 µg), and 24 h after CCl₄ injection (250 µg) as described in a previous study,¹⁰ and animals were sacrificed 48 h after CCl₄ injection.

Histological analysis

Immunohistochemical analysis was performed on formalin-fixed paraffin-embedded mouse or human liver sections (4 µm). To study hepatocyte proliferation and apoptosis, immunostaining was performed using anti-bromodeoxyuridine (BrdU; 1:40, Abcam ab6326), anti-phospho-histone H3 (PHH3; 1:1,000, EMD Millipore 06-570), anti-Ki67 (1:100, Dako M7240), and a cleaved caspase-3 (Asp175) (1:50, Cell Signaling Technology, Danvers,

Table 1. Patient characteristics for precision-cut liver slices study.

Patient	Age (years)	Sex	Reason and type of surgery	Aetiology of fibrosis	METAVIR or SAF score
1	61	M	HCC (explanted liver)	Alcohol	A0F4
2	51	M	Decompensated cirrhosis (explanted liver)	Alcohol	A0F4
3	74	F	HCC (resected liver)	Metabolic	S1A4F3
4	68	M	HCC (explanted liver)	Alcohol and metabolic	S0A0F4
5	68	F	Decompensated cirrhosis (explanted liver)	Metabolic	S1A3F4
6	81	F	CC (resected liver)	Metabolic	S1A1F2
7	69	M	HCC (resected liver)	Alcohol and metabolic	S1A1F3/F4

CC, cholangiocarcinoma; F, female; HCC, hepatocellular carcinoma; M, male; SAF, steatosis, activity, fibrosis.

MA, USA, 9661) antibodies. Anti-rat (Vector Laboratories BA-9401) or anti-rabbit antibody (Bio-Rad STAR131B) was used as a secondary antibody. The signal was enhanced using the Vectastain Elite ABC kit (Vector Laboratories PK-6100) and revealed by the 3,3'-Diaminobenzidine kit (Dako K3468) according to the manufacturer's instructions. Images were taken at 20× magnification. Positive hepatocytes were counted blindly by two independent observers on 15 fields using ImageJ software in mice and 8 fields in human sections (4,000–8,000 hepatocytes). No staining was observed when the primary antibody was omitted.

RNA sequencing

RNASeq was performed as previously described.^{11–16} Genes were considered as expressed if their FPKM (fragments per kilobase per million mapped fragments) value was greater than 95% of the background FPKM value based on intergenic regions defined from the Mouse FAST DB v2018_1 annotations. Differential gene expression analysis was performed using DESeq2, and results were considered statistically significant for *p* values ≤0.05 and fold changes ≥1.5. Enrichment tests were performed using WebGestaltR¹⁷ from Kyoto Encyclopedia of Genes and Genomes (KEGG), Gene Ontology (GO), and Reactome databases with cut-off values of *p* <0.05 and a minimum of two overlapping genes. The sequence datasets have been deposited in the Gene Expression Omnibus with the accession number GSE 189064. For more details, see Supplementary information.

Statistical analysis

All statistical analyses were performed with Prism software 8.4.3 (GraphPad Software, Inc., La Jolla, CA, USA) using the nonparametric Mann–Whitney *U* test or a paired *t* test as indicated in figure legends. Data are presented as mean ± SD, and *p* ≤0.05 was considered statistically significant. Sample sizes were adequate to detect effects between groups, as determined by the reproducibility and variability of each experiment.

Study approval

Experiments were performed in accordance with protocols approved by the French Ministère de l'Enseignement Supérieur de la Recherche et de l'Innovation (project authorisation using animals for scientific purposes APAFIS #30284-2021030912208867).

For western blots, reverse-transcription PCR ELISA, and *in vitro* studies, see Supplementary information.

Results

Inhibition of MAGL limits hepatocyte proliferation *ex vivo* in human PCLS and *in vitro* in human hepatoma cell lines

To investigate the impact of MAGL inhibition on hepatocyte proliferation, we first took advantage of the differential expression of MAGL in the human hepatoma HuH7 and HuH6 cell lines (Fig. 1A). We observed that the pharmacological MAGL inhibitor MJN110 reduces DNA synthesis in the MAGL-expressing HuH7 cell line, whereas it had no effect in the MAGL-deficient HuH6 cell line (Fig. 1B).

We then exposed PCLS from patients with chronic liver injury (Table 1) to MJN110, or its vehicle, for 48 h. The proportion of Ki67-positive hepatocytes was significantly reduced after MJN110 exposure compared with control (Fig. 1C and D). Only one PCLS coming from the non-tumoural liver with mild fibrosis of a patient with cholangiocarcinoma showed no reduced proliferation.

These results demonstrate that MAGL inhibition negatively impacts hepatocyte proliferation. We therefore further explored the role of MAGL in mouse models of liver regeneration.

MAGL promotes liver regeneration

We investigated the impact of MAGL inactivation in experimental mouse models as induced by an acute CCl₄ administration (Fig. 2A) or a two-thirds PHx (Fig. 2B). We compared the regeneration kinetics of wild-type (WT) mice, global MAGL-inactivated mice (MAGL^{-/-}), or mice exposed to the pharmacological inhibitor MJN110 before injury. Both models of MAGL inactivation showed a significant reduction in BrdU incorporation and PHH3 hepatocyte immunostaining 48 and 72 h after toxic liver injury, compared with controls (Fig. 2A and B). Moreover, at the same time points, cyclin A was expressed at substantially lower levels in MAGL^{-/-} and MJN 110-treated mice than in their control counterparts (Fig. 3A and B). Interestingly, cyclin D1 expression was already reduced 30 h after CCl₄ injection in MAGL-inhibited mice (Fig. 3A and B). Altogether, these results demonstrated that global inactivation delayed liver regeneration. In line with the known hepatoprotective effects of MAGL inhibitors,⁸ reduced serum transaminase levels and decreased necrotic area were found in MJN110-treated and MAGL^{-/-} mice compared with their respective controls after an acute CCl₄ injection (Fig. S1A and B). To determine whether MAGL defect impacts liver regeneration independently of its hepatoprotective effect, we performed two-thirds PHx. Survival

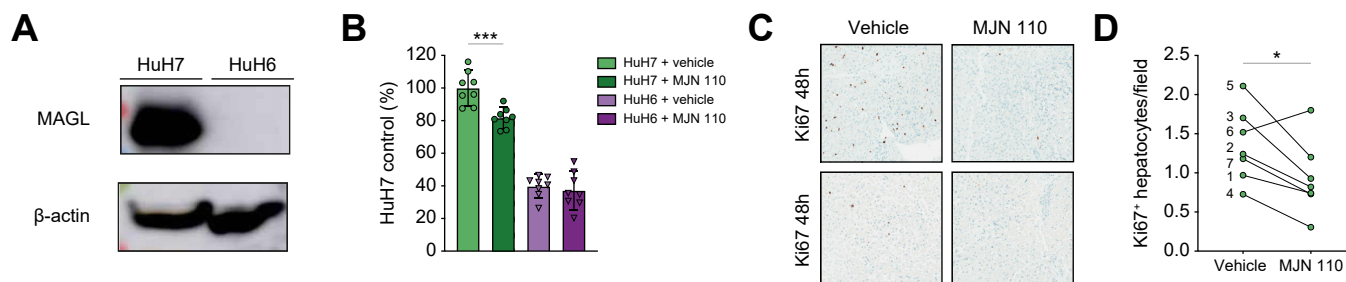


Fig. 1. MAGL inhibition with MJN110 reduces hepatocyte proliferation in human hepatoma cell lines and PCLS from patients with chronic liver disease. (A) Western blot of MAGL expression in human hepatoma cell lines HuH7 and HuH6. β-actin was used as a loading control. (B) Quantification of DNA synthesis in human hepatoma cell lines exposed to MJN110 or its vehicle, expressed as a percentage of HuH7 + vehicle proliferation (representative of three experiments). ****p* <0.001, by two-tailed Mann–Whitney *U* test. Human PCLS were incubated with 10 μM MJN110 or vehicle for 48 h: (C) representative images of Ki67-immunostained PCLS sections treated with MJN110 or its vehicle as indicated (magnification, 20×) and (D) quantification of Ki67-positive hepatocytes per field. **p* <0.05, non-parametric Wilcoxon paired test. For patient numbers, refer to Table 1. MAGL, monoacylglycerol lipase; PCLS, precision-cut liver slices.

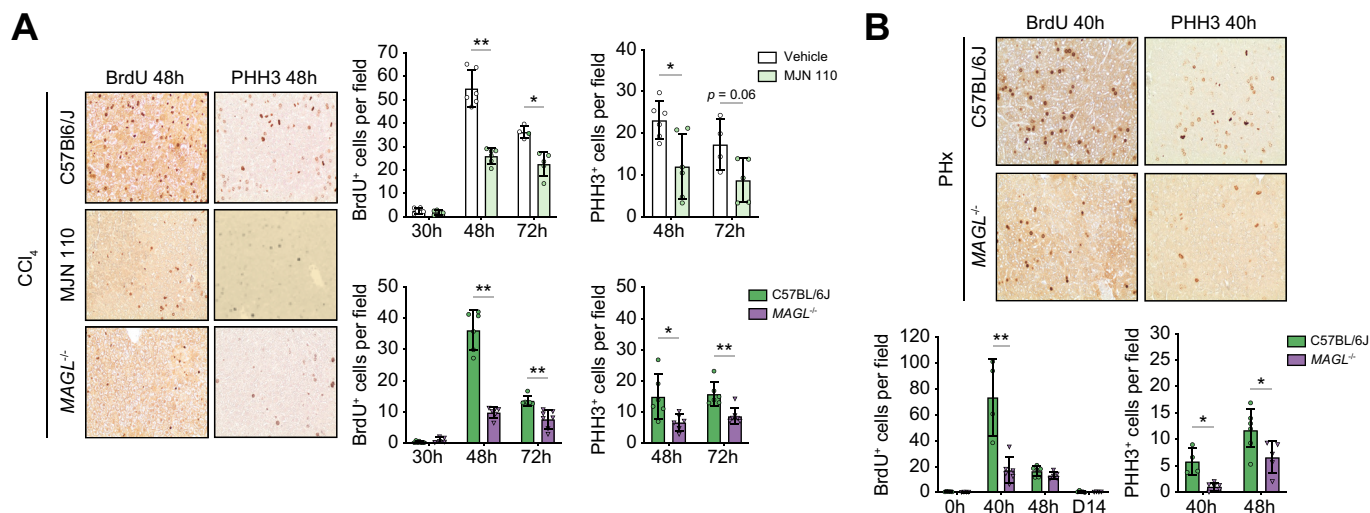


Fig. 2. MAGL invalidation or inhibition delays liver regeneration. Representative liver sections of BrdU- and PHH3-stained hepatocytes in C57BL/6J mice, MAGL^{-/-} mice, and MJN110-treated mice (A) 48 h after CCl₄ injection and (B) 40 h after PHx. Corresponding quantifications of BrdU- and PHH3-stained hepatocytes are shown at indicated time points after injury (n = 5–7 mice per group). BrdU, bromodeoxyuridine; CCl₄, carbon tetrachloride; MAGL, monoacylglycerol lipase; PHH3, phospho-histone H3; PHx, partial hepatectomy. *p > 0.05, **p < 0.01 by two-tailed Mann-Whitney U test.

was higher than 90% and independent of the genotype. In this model, the level of injury was very low, and there was no difference in either necrosis or apoptosis, as assessed by aspartate aminotransferase–alanine aminotransferase levels, necrotic area, and cleaved caspase-3-stained hepatocyte quantification between MAGL^{-/-} and WT mice (Fig. S1C). We observed a delay in liver mass recovery upon MAGL global deletion 14 days after PHx at a time point where the liver weight on body weight (LW/BW) ratio of control livers is restored (Fig. S2A). A reduction in BrdU incorporation and PHH3 hepatocyte staining was observed at the peak of proliferation (*i.e.* 40 h) after surgical resection in mutated animals compared with controls (Fig. 2B). This was confirmed by a reduction in cyclin A expression in mutant mice (Fig. 3C and S2B).

Hepatocyte-specific invalidation of MAGL impairs hepatocyte proliferation owing to a reduced eicosanoid production

We then investigated the contribution of MAGL in hepatocytes and macrophages to the liver regeneration process. We first generated mice lacking MAGL specifically in hepatocytes (MAGL^{Hep-/-}) by crossing MAGL^{fl/fl} with transgenic mice expressing Cre recombinase under the control of the albumin promoter. The deletion efficacy was confirmed by the decrease in MAGL expression in the total liver and primary hepatocytes (Fig. S2C). We showed a reduced hepatocyte proliferation at the peak, that is, 48 h after CCl₄ injection (Fig. S2D). However, as for MAGL global deletion, hepatocyte MAGL deficiency protected against acute injury as shown by the reduced aspartate aminotransferase levels (Fig. S2D). To determine whether MAGL hepatocyte-specific deficiency delayed regeneration independently of liver injury, we performed PHx. We observed a delayed recovery of LW/BW ratio 14 days after surgery (Fig. S2A). Importantly, there was a reduced hepatocyte BrdU staining in MAGL^{Hep-/-} animals compared with their respective MAGL^{fl/fl} controls with a reduced cyclin A expression (Fig. 4A and B) 40 and 48 h after surgery. The cell-intrinsic proliferative impact of MAGL was investigated in isolated primary hepatocytes. MAGL-

deficient hepatocytes showed a reduced proliferation rate as compared with control C57BL/6J hepatocytes (Fig. 4C). Moreover, as in human hepatocytes, MJN110 reduced the proliferation of primary hepatocytes from WT C57BL/6J mice, whereas it had no impact on MAGL-invalidated hepatocytes (Fig. 4C). Taken together, these data demonstrate that *in vitro* as well as *in vivo* inhibition of MAGL in hepatocytes reduces their proliferation.

Pharmacological inhibition of MAGL leads to a decrease in arachidonic acid-derived metabolites, among which are prostaglandin E₂ (PGE₂) and thromboxane A₂ (TXA₂), two important mediators in hepatocyte growth and liver regeneration.^{18–21} PGE₂ was constitutively reduced in total liver extracts of MAGL^{-/-} and MAGL^{Hep-/-} mice compared with their respective controls already at basal levels (Fig. 4D). Pharmacological inhibition of MAGL by MJN110 reduced PGE₂ production by control primary hepatocytes, but it had no effect on MAGL^{-/-} hepatocytes (Fig. 4E). In keeping with this finding, primary hepatocytes isolated from MAGL^{-/-} mice showed reduced proliferation compared with control C56BL/6J hepatocytes, and this negative impact on proliferation was overcome by exogenous addition of PGE₂ in the culture medium (Fig. 4F). Other metabolites of the arachidonic pathway could have also supported hepatocyte proliferation. In keeping with this hypothesis, we also found a reduced TXA₂ production in MAGL^{Hep-/-} livers at basal levels and during regeneration as well as in invalidated hepatocytes or control hepatocytes treated with MJN110 (Fig. S2E). Altogether, these data support an intrinsic pro-regenerative impact of MAGL that is mediated via eicosanoid production.

Macrophage MAGL deficiency impairs liver regeneration and reprograms macrophage signature towards an IFN-1 pathway

To determine the contribution of MAGL from macrophages to liver repair, we used mice lacking MAGL in the myeloid lineage (MAGL^{Mye-/-}). The invalidation of MAGL was confirmed in bone marrow-derived macrophages (BMDM) (Fig. S2C). Impaired liver regeneration was observed in MAGL^{Mye-/-} mice after CCl₄ acute injury (Fig. 5A and B). Importantly, in contrast to that in MAGL

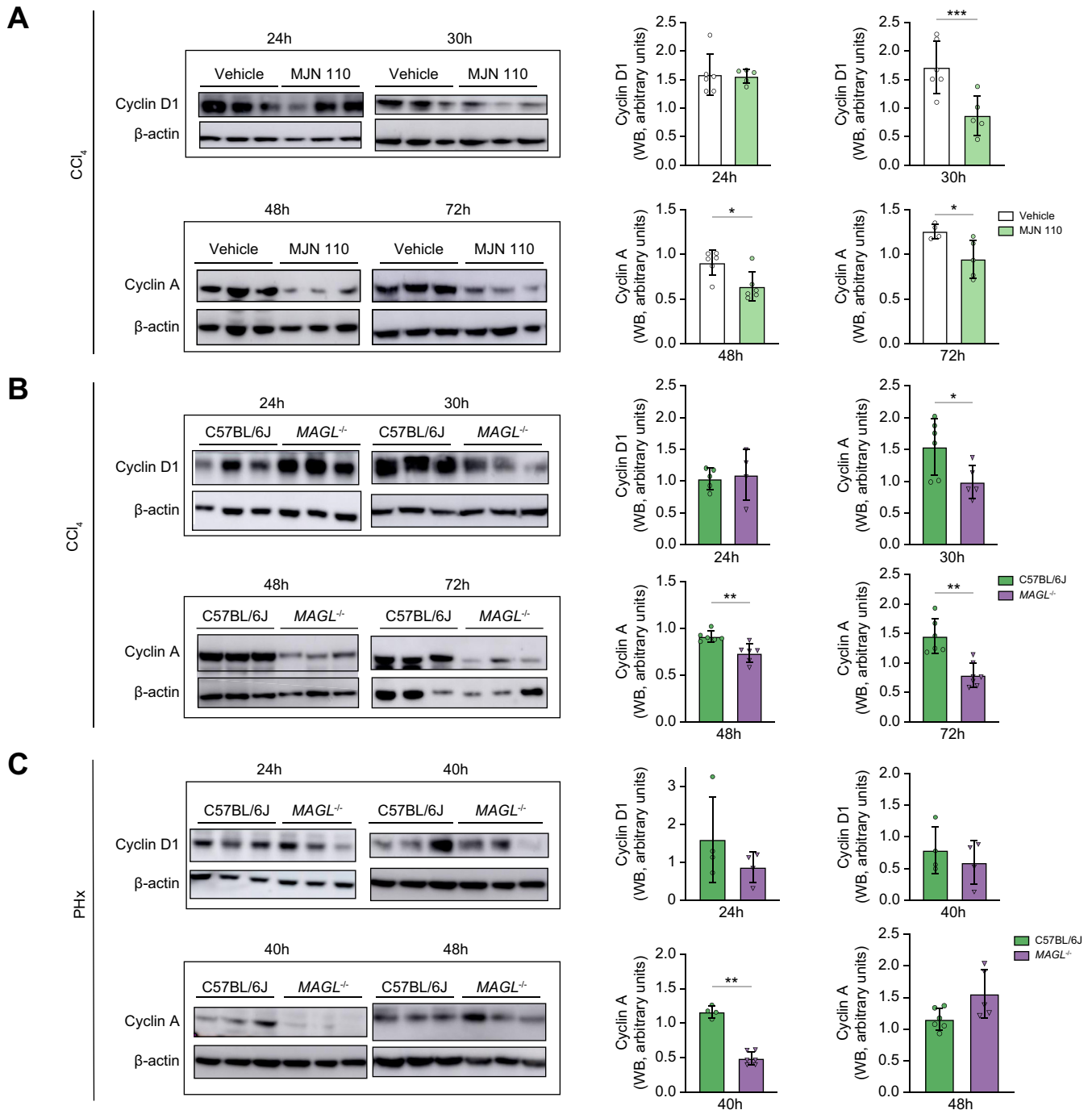


Fig. 3. MAGL invalidation or inhibition reduces hepatocyte proliferation during liver regeneration. Western blot analysis of liver cyclin D1 and cyclin A expression with corresponding quantifications at indicated time points in (A) C57BL/6J mice treated with vehicle or MJN110 after CCl₄ injection, (B) C57BL/6J and MAGL^{-/-} mice after CCl₄ injection, and (C) C57BL/6J and MAGL^{-/-} mice after PHx (n = 5–7 mice per group). β-actin was used as a loading control. *p < 0.05, **p < 0.01, by two-tailed Mann–Whitney U test. CCl₄, carbon tetrachloride; MAGL, monoacylglycerol lipase; PHH3, phospho-histone H3; PHx, partial hepatectomy; WB, western blot.

Hep^{-/-} mice, there was no reduction in cell death in MAGL^{Mye^{-/-}} mice compared with their MAGL^{fl/fl} control counterparts at the peak of injury (Fig. S3A). These results demonstrated that MAGL inhibition in macrophages delays regeneration independently of liver injury.

Macrophages are known to be essential in liver regeneration noteworthy by producing cytokines such as IL-6 and tumour

necrosis factor α (TNF-α) in a few hours following a regeneration stimulus, allowing the hepatocytes to become responsive to growth factors.² Acute liver damage is accompanied by a massive recruitment of immune cells and particularly macrophages that play a major role in liver regeneration.²² We did not observe any reduction in IL-6 or TNF-α expression in the liver of invalidated mice after an acute injury (Fig. S3B). Flow cytometry analysis of

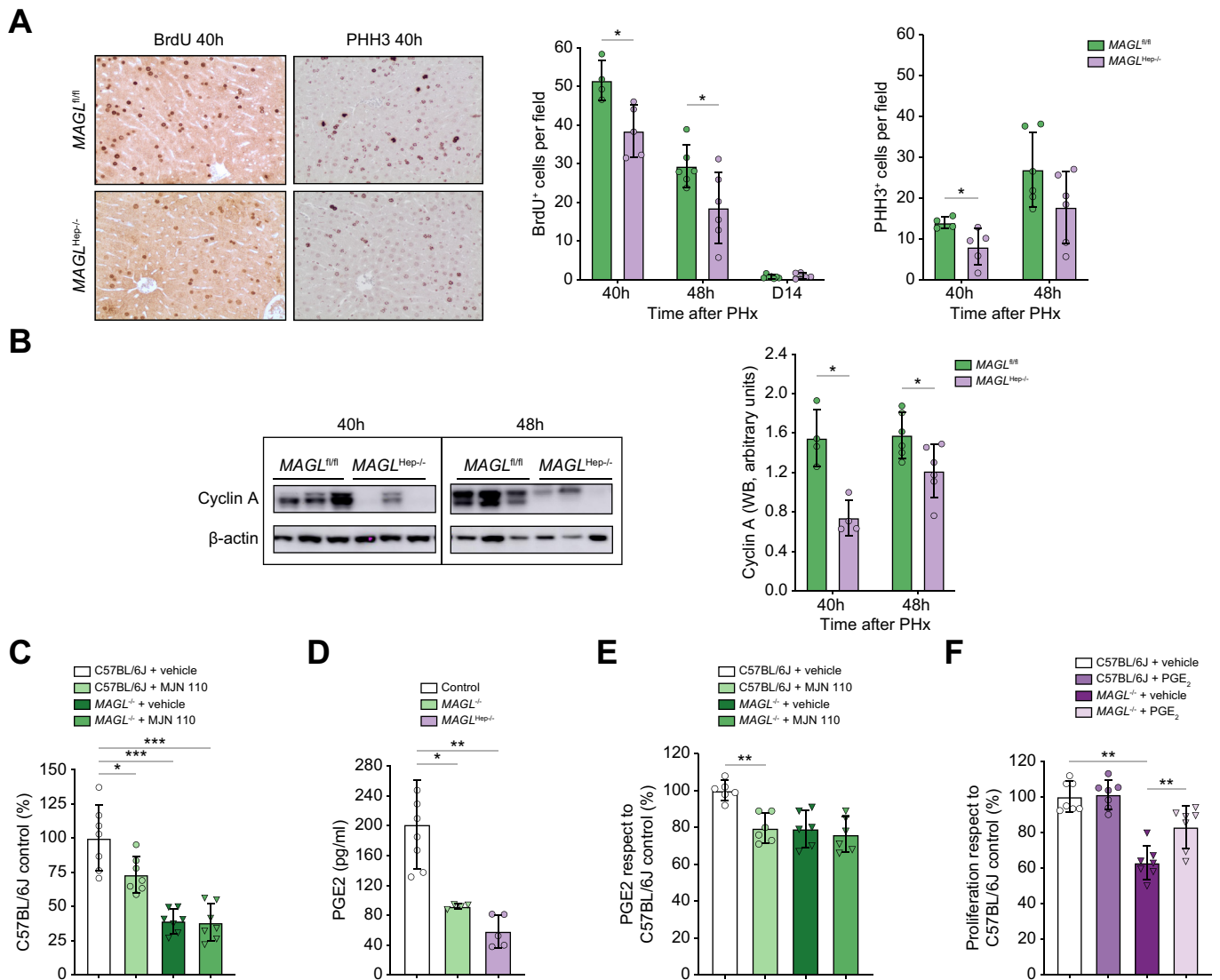


Fig. 4. Hepatocyte-specific MAGL invalidation impacts hepatocyte proliferation *in vivo* and *in vitro* owing to a reduced eicosanoid production. (A) Representative liver sections 40 h after PHx and respective quantification of BrdU- and PHH3-positive hepatocytes in MAGL^{Hep-/-} compared with MAGL^{fl/fl} controls at indicated time points (n = 4–6 mice per group). (B) WB analysis and corresponding quantification of cyclin A expression, 40 and 48 h after PHx in MAGL^{Hep-/-} and MAGL^{fl/fl} (n = 4–6 mice per group). β -actin was used as a control. (C) Quantification of DNA synthesis in primary hepatocytes isolated from C57BL/6J and MAGL^{-/-} mice exposed to vehicle or to MJN110, expressed as a percentage of control proliferation (C57BL/6J + vehicle). Representative of three experiments. (D) PGE₂ quantification assayed by ELISA in the liver of MAGL^{-/-} and MAGL^{Hep-/-} mice and their respective controls. (E) PGE₂ quantification assayed by ELISA in primary hepatocytes isolated from C57BL/6J and MAGL^{-/-} mice exposed to MJN110 or its vehicle for 48 h as indicated (three experiments) expressed as a percentage of C57BL/6J vehicle-treated hepatocytes. (F) Quantification of DNA synthesis in primary hepatocytes isolated from C57BL/6J and MAGL^{-/-} mice exposed to vehicle or to PGE₂ for 48 h expressed as a percentage of control hepatocyte proliferation (C57BL/6J + vehicle). Representative of three experiments. * $p < 0.05$, ** $p < 0.01$, *** $p < 0.001$, by two-tailed Mann–Whitney *U* test. BrdU, bromodeoxyuridine; MAGL, monoacylglycerol lipase; PGE₂, prostaglandin E₂; PHH3, phospho-histone H3; PHx, partial hepatectomy; WB, western blot.

total liver immune cells at the peak of injury revealed that the percentage of CD4⁺ and CD8⁺ T lymphocytes, natural killer cells, natural killer T cells, $\gamma\delta$ T cells, or macrophages (Fig. 5C) was not affected by MAGL deletion in myeloid cells, although a reduced macrophage population was observed at a later time point (Fig. S3C). Moreover, the recruitment of pro-inflammatory Ly6C^{High} macrophages was similarly induced in MAGL^{fl/fl} and MAGL^{Mye-/-} mice at the peak of liver injury, that is, 24 h after injury as assessed by FACS (Fig. 5C) and immunohistochemistry (Fig. S3C). We measured eicosanoids in the liver in basal conditions and after injury and found no significant difference

between control and MAGL^{Mye-/-} mice (Fig. S3D). However, we cannot exclude from these data that a reduced production of PGE₂ and/or TXA₂ expression by macrophages might contribute to the delay in liver regeneration.

To further explore the link between MAGL inactivation in macrophages and liver regeneration, we performed an RNASeq analysis on F4/80⁺CD11b⁺ macrophages sorted from the liver of MAGL^{Mye-/-} and MAGL^{fl/fl} mice 24 h after CCl₄ injection (Fig. S3E). We found that 549 genes were differentially expressed with 323 upregulated and 226 downregulated in MAGL^{Mye-/-} macrophages compared with MAGL^{fl/fl} macrophages (Fig. 6A). As anticipated,

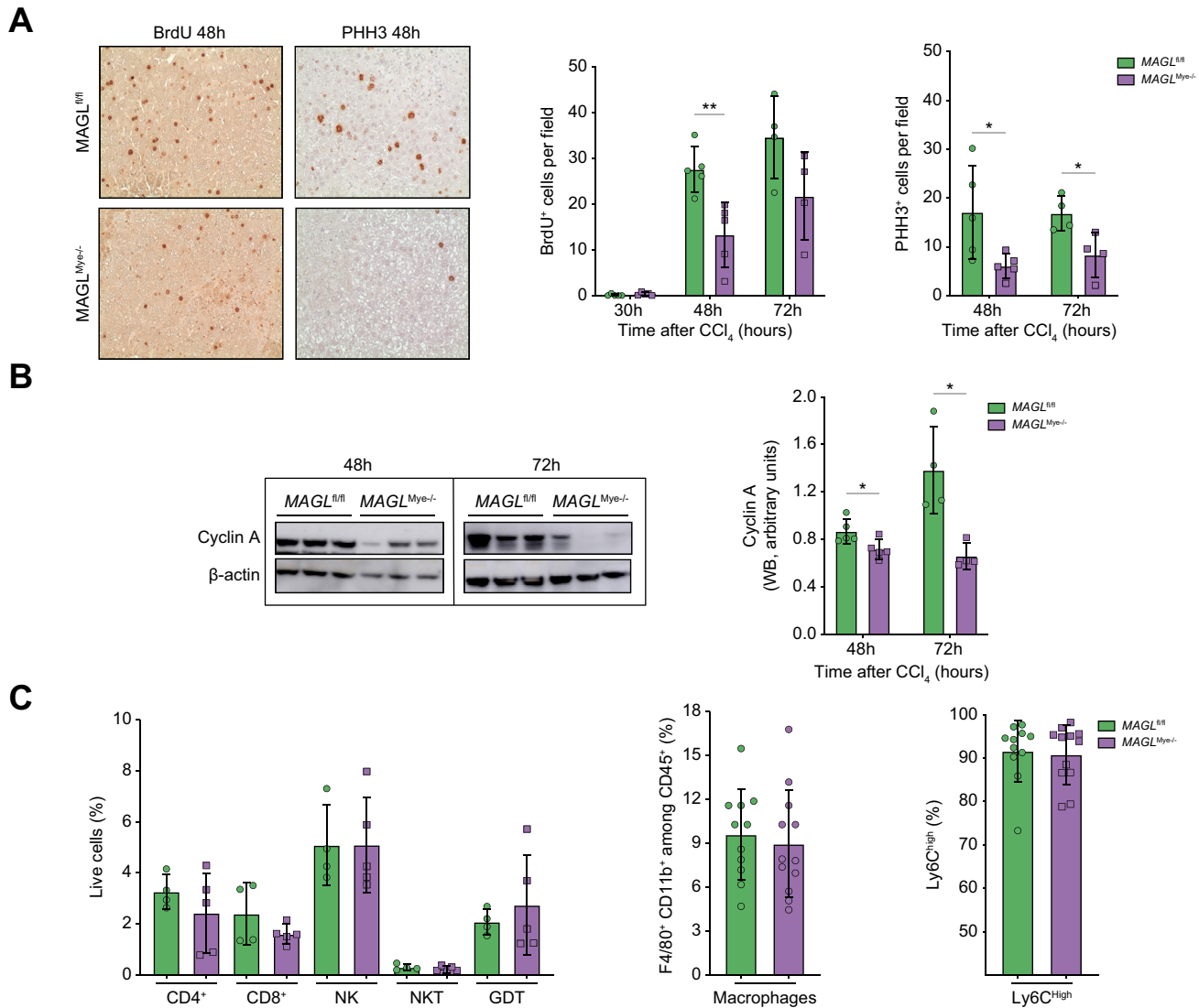


Fig. 5. Myeloid-specific MAGL invalidation delays liver regeneration without modulating macrophage recruitment. (A) Representative liver sections of BrdU- and PHH3-stained hepatocytes in C57BL/6J, MAGL^{fl/fl}, and MAGL^{Mye-/-} mice 48 h after CCl₄ injection. Corresponding quantifications of BrdU- and PHH3-stained hepatocytes at indicated time points after injury (n = 5–7 mice per group). (B) WB analysis of liver cyclin A expression with corresponding quantifications are reported to their respective controls at indicated time points after CCl₄ injection (n = 5–7 mice per group). β-actin was used as a loading control. *p < 0.05, **p < 0.01, by two-tailed Mann–Whitney U test. (C) Flow cytometry analysis of the frequency of LT, NK, NKT (TCRb⁺ NK1.1⁺), GDT, macrophages (F4/80⁺CD11b⁺), and Ly6C^{high} macrophages sorted from MAGL^{fl/fl} and MAGL^{Mye-/-} mice, 24 h after CCl₄ injection (representative of two experiments). *p < 0.05, **p ≤ 0.01, by two-tailed Mann–Whitney U test. BrdU, bromodeoxyuridine; CCl₄, carbon tetrachloride; GDT, γδ T cells; LT, T lymphocytes; MAGL, monoacylglycerol lipase; NK, natural killer cells; NKT, natural killer T cells; PHH3, phospho-histone H3; WB, western blot.

modulation of the eicosanoid pathway was observed, with upregulation of genes upstream of MAGL such as diacylglycerol kinase, phospholipase D2, or lipin-2 in MAGL^{Mye-/-} mice and downregulation of genes downstream of MAGL such as prostaglandin E receptor 2 or prostaglandin E synthase 3-like. Classical pro-inflammatory and pro-regenerative cytokines, such as IL-6 or TNF-α, were not differentially expressed in MAGL^{Mye-/-} mice as compared with their WT counterparts. However, GO analysis of biological functions associated with the differentially expressed genes revealed that 5 of the 10 first Reactome deregulated pathways were related to IFN-I (Fig. 6B), a vast majority of genes being upregulated in MAGL^{Mye-/-} macrophages. A gene set enrichment analysis performed on four GO terms linked to the IFN-I pathway confirmed the enrichment in this

gene signature pathway (Figs. 6C and Fig. S4A). The induction of some interferon (IFN)-stimulated gene expression such as *Eif2ak2*, *IRF7*, and *Ifit3* was confirmed in BMDM isolated from CCl₄-injected MAGL^{Mye-/-} mice as compared with their MAGL^{fl/fl} counterparts (Fig. S4B).

The deleterious impact of IFN-I pathway induction on hepatocyte proliferation and liver regeneration

To determine whether the induction of the IFN-I pathway was responsible for the liver regeneration defect, we cultured primary hepatocytes in the presence of IFN-α, IFN-β, or both and observed a reduction in hepatocyte proliferation with a cumulative effect of IFN-α and IFN-β (Fig. 6D). The detrimental impact of IFN-I pathway induction was further demonstrated in an

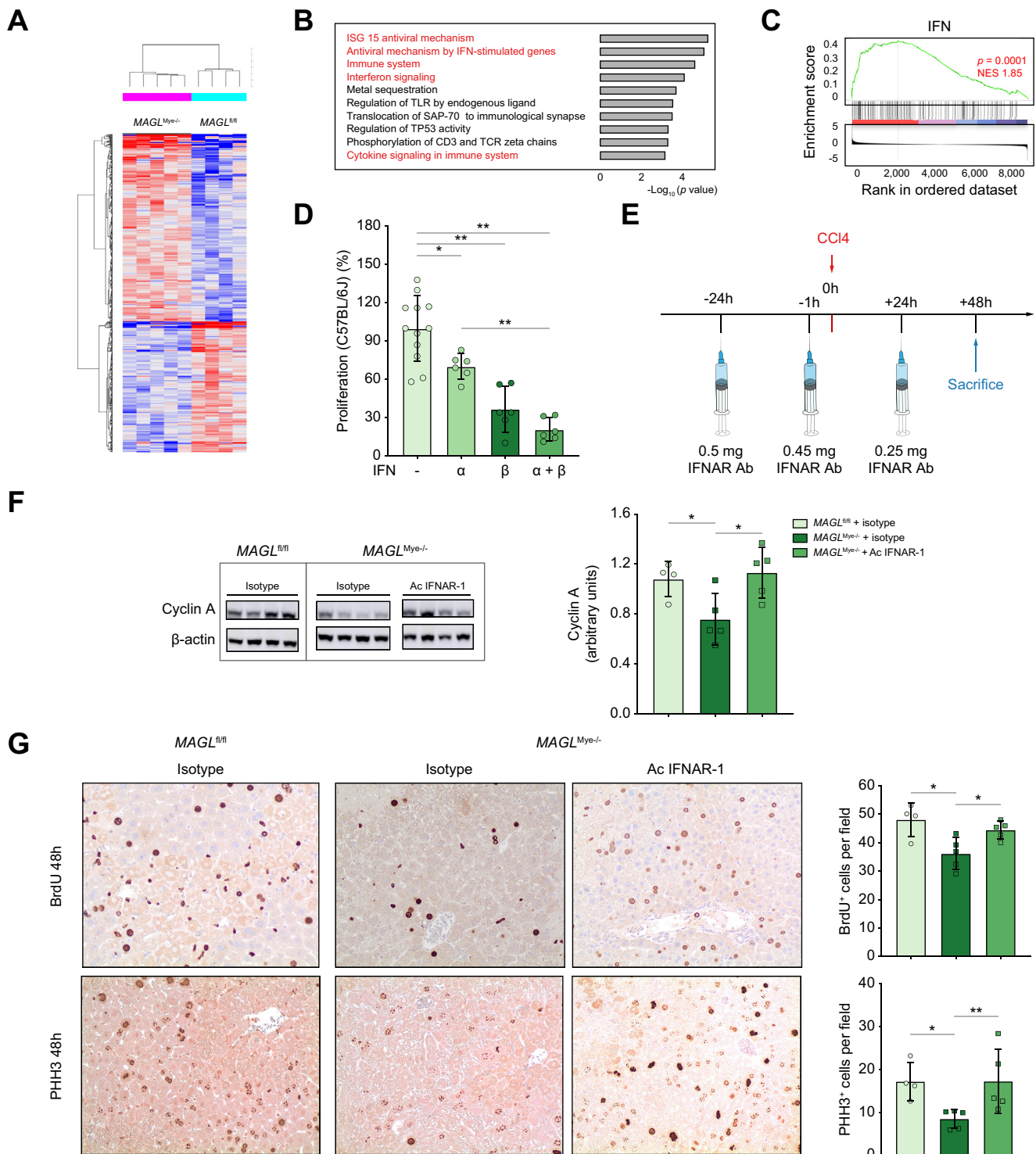


Fig. 6. MAGL deletion reprograms macrophage signature towards IFN-I pathway profile that reduces hepatocyte proliferation. (A) Heatmap of differentially expressed genes between liver macrophages sorted from MAGL^{Mye-/-} and MAGL^{fl/fl} mice 24 h after CCl₄ injection. (B) Top 10 Reactome pathways ordered by $-\log_{10}$ (p value) (Fisher's exact test). Pathways related to IFN-I are indicated in red. (C) GSEA demonstrating specific enrichment for an IFN-I signature in the gene expression profile of MAGL^{Mye-/-} macrophages (custom GSEA module defined with genes from Gene Ontology GO:0032606, GO:0034340, GO:0035455, and GO:0035456). (D) Proliferation index of control C57BL/6J primary hepatocytes treated with IFN- α , IFN- β , or both, expressed in percentage of non-treated hepatocyte proliferation index (representative of two experiments). (E) Schematic of study design for mice receiving Ac IFNAR-1 antibody or isotype (24 h before, 1 h before, and 24 h after CCl₄ injection). Mice were harvested 48 h after CCl₄ injection. (F) Western blot of liver cyclin A expression and respective quantification in MAGL^{fl/fl} mice exposed to isotype antibody and MAGL^{Mye-/-} mice exposed to Ac IFNAR-1 or isotype 48 h after CCl₄ injection. β -actin was used as a loading control. (G) Representative BrdU- and PHH3-immunostained liver sections and respective quantification in MAGL^{Mye-/-} mice exposed to Ac IFNAR-1 or isotype compared with their MAGL^{fl/fl} counterparts, 48 h after CCl₄ injection. * $p < 0.05$, ** $p < 0.01$, by two-tailed Mann-Whitney U test. BrdU, bromodeoxyuridine; CCl₄, carbon tetrachloride; GSEA, gene set-enrichment analysis; IFN, interferon; IFN-I, type I interferon; IFNAR, interferon α/β receptor; MAGL, monoacylglycerol lipase; NES, normalised enrichment score; PHH3, phospho-histone H3; TCR, T-cell receptor; TLR, Toll-like receptor.

in vivo rescue experiment with neutralising antibodies against IFN-I receptor compared with the isotype injected to MAGL^{Mye^{-/-}} (Fig. 6E). Importantly, IFN-I inhibition restored cyclin A expression (Fig. 6F) and hepatocyte proliferation (Fig. 6G) to the level of control mice, indicating that IFN-I induction in myeloid cells underlies the liver regeneration defect in MAGL^{Mye^{-/-}} mice.

Discussion

Liver regeneration is an instrumental process that allows restoring tissue architecture and function following acute physical or toxic liver injury. Well-established timely orchestrated cellular and molecular responses occur to promote liver regeneration.² These processes involve inflammatory reactions and metabolic changes that take place not only in hepatocytes but also in environmental immune cells and particularly in macrophages.¹⁻³ However, the same pathways that promote liver regeneration, when chronically stimulated, may result in an imbalance driving fibrosis. This illustrates the delicate equilibrium that exists between liver regeneration and fibrosis.^{23,24} Changes in lipid metabolism also contribute to fibrosis progression through the control of immune cells, hepatocyte damage, and activation of fibrogenic cells.²⁵ Recently, we identified MAGL as a pro-fibrogenic enzyme, and we demonstrated that MAGL inhibitors are promising anti-fibrogenic compounds that could even drive fibrosis regression.⁸ Interestingly, MAGL inactivation specifically in myeloid cells was sufficient to reduce inflammation and fibrosis progression upon chronic liver injury.⁸ We hypothesised that MAGL inhibition could also affect liver regeneration. Combining human data in PCLS and various models of MAGL inactivation, the present study demonstrates that inhibiting MAGL reduces hepatocyte proliferation *in vitro* and *ex vivo* and delays liver regeneration.

Inhibition of MAGL leads to an increase in 2-arachidylglycerol production,⁸ which activates cannabinoid receptors 1 (CB1) and 2 (CB2). We have shown that CB1 or CB2 activation promotes liver regeneration through increased production of IL-6 from hepatic myofibroblasts for CB2²⁶ and activation of cell cycle proteins involved in mitotic progression such as forkhead-box M1 for CB1.²⁷ It is therefore most likely that the delayed liver regeneration induced by MAGL inactivation is not mediated by cannabinoid receptors.

MAGL-specific deletion in hepatocytes was associated with a defect in liver regeneration and a lower production of PGE₂ both *in vivo* and *in vitro*. Among metabolites of arachidonic acid, PGs, including PGE₂, the most abundant PG produced by the liver,²⁸ and prostacyclin (prostaglandin I₂), are known to promote the growth of hepatocytes.^{19,20,29-31} Moreover, inhibition of 15-prostaglandin dehydrogenase, a PG-degrading

enzyme, has been shown to potentiate tissue regeneration in multiple organs in mice, including the liver.³² Interestingly, addition of PGE₂ in the culture medium of MAGL^{Hep^{-/-}} hepatocytes rescued their proliferation, suggesting a cell-intrinsic impact of PGE₂ on hepatocyte proliferation and liver regeneration. Among other metabolites of the arachidonic pathway that could also support hepatocyte proliferation, TXA₂ also promotes liver regeneration.^{19,21,22} As TXA₂ was also down-regulated in MAGL-inactivated hepatocytes, it is likely that it also contributes to the liver regeneration delay. Thus, our data uncover the beneficial pro-regenerative effect of MAGL expressed by hepatocytes on their proliferation through eicosanoid production.

Immune cells, in particular macrophages, play a major role in the early phase of the regeneration process, particularly through their cytokine production.² We found that mice specifically inactivated for MAGL in the myeloid lineage also show a defective liver regeneration. Unexpectedly, intrahepatic macrophages from MAGL^{Mye^{-/-}} mice, unlike MAGL^{Mye^{-/-}} BMDMs upon lipopolysaccharide stimulation, do not express lower levels of pro-inflammatory and pro-regenerative cytokines 24 h after liver injury. However, we demonstrated that MAGL inactivation in macrophages has indeed an indirect early negative impact on hepatocyte proliferation through the induction of the IFN-I pathway, underlining a novel mechanism by which MAGL deletion reprograms macrophages. These results are in keeping with data showing reduced hepatocyte proliferation upon addition of IFN-I *in vitro* or *in vivo* during regeneration.^{33,34} More importantly, liver regeneration was rescued by *in vivo* blockade of IFN-I pathway in MAGL^{Mye^{-/-}} mice, underlining its major role in the liver regeneration delay observed in the absence of MAGL in myeloid cells. Interestingly, reduced eicosanoid production has been correlated with IFN-I induction by macrophages upon viral infection.³⁵ Although PGE₂ and TXA₂ was not reduced in the liver of MAGL^{Mye^{-/-}} mice, liver and peritoneal MAGL-deleted macrophages are known to produce less eicosanoids.⁸ Therefore, reduced PGE₂ production may also link the MAGL defect in macrophages and the IFN-I pathway induction observed in our model.

In conclusion, our results highlight the regenerative properties of MAGL in the liver, via both an intrinsic lipid reprogramming of hepatocytes and an extrinsic reprogramming of macrophages that turns off the IFN-I pathway and induces a macrophage-hepatocyte crosstalk. Owing to the balance between fibrogenesis and regeneration, these data illustrate that the price to pay when using MAGL inhibitors as an anti-inflammatory and anti-fibrogenic strategy is to compromise liver regeneration.

Abbreviations

2-AG, 2-arachidylglycerol; BMDM, bone marrow-derived macrophages; BrdU, bromodeoxyuridine; BW, body weight; CB1, cannabinoid receptor 1; CB2, cannabinoid receptor 2; CC, cholangiocarcinoma; CCl₄, carbon tetrachloride; FPKM, fragments per kilobase per million mapped fragments; GO, Gene Ontology; GSEA, gene set enrichment analysis; HCC, hepatocellular carcinoma; IFN, interferon; IFN-I, type I interferon; IFNAR, interferon α/β receptor; i.p., intraperitoneally; KEGG, Kyoto Encyclopedia of Genes and Genomes; LW/BW, liver weight on body weight; MAGL, monoacylglycerol lipase; NES, normalised enrichment score; PCLS, precision-cut liver slices; PG, prostaglandin; PGE₂, prostaglandin E₂; PHH3,

phospho-histone H3; PHx, partial hepatectomy; RNASeq, RNA sequencing; SAF, Steatosis, Activity, Fibrosis; TNF- α , tumour necrosis factor α ; TXA₂, thromboxane A₂; WB, western blot; WT, wild-type.

Financial support

This work was supported by grants from INSERM (France), Agence Nationale pour la Recherche (ANR 20-CE14-0038), the University de Paris Labex Inflammex, Fondation pour la Recherche Médicale (Equipe FRM EQU202203014642), Association Française pour l'Etude du Foie (AFEF), and Société Nationale Française de Gastroentérologie (SNFGE). MA was a

recipient of a doctoral fellowship from INSERM poste d'accueil. MS was a recipient of FRM fellowship.

Conflicts of interest

The authors have declared that no conflict of interest exists regarding this work.

Please refer to the accompanying ICMJE disclosure forms for further details.

Authors' contributions

Study concept and design: HG, SL. Acquisition of data: MA, RAS, MM, MC, JHW, PG, AH, CC. Surgery: MS. Analysis and interpretation of data: MA, RAS, MM, MC, JHW, A Habib, VP, SL, HG. Drafting of the manuscript: MA, PG, SL, HG. Study supervision: HG. Critical revision of the manuscript: SL, MLG, CP, VP.

Data availability statement

The data that support the findings of this study are available from the corresponding authors upon reasonable request.

Acknowledgements

The authors thank V. Fauveau, Institut Cochin, for help in surgery experiments; Olivier Thibaudeau of the Plateau de Morphologie Facility (INSERM UMR 1152, France) and Nicolas Sorhaindo of the Plateforme de Biochimie (CRI, INSERM UMR1149) for their help in the histology and liver function tests; and K. Bailly from the cytometry platform of Cochin Institute and H. Fohrer-Ting from the Centre de Recherche des Cordeliers, Paris University, for cell sorting analyses.

Supplementary data

Supplementary data to this article can be found online at <https://doi.org/10.1016/j.jhepr.2023.100794>.

References

Author names in bold designate shared co-first authorship

- [1] Huang J, Rudnick DA. Elucidating the metabolic regulation of liver regeneration. *Am J Pathol* 2014;184:309–321.
- [2] Michalopoulos GK, Bhushan B. Liver regeneration: biological and pathological mechanisms and implications. *Nat Rev Gastroenterol Hepatol* 2021;18:40–55.
- [3] Solhi R, Lotfinia M, Gramignoli R, Najimi M, Vosough M. Metabolic hallmarks of liver regeneration. *Trends Endocrinol Metab* 2021;32:731–745.
- [4] Dinh TP, Carpenter D, Leslie FM, Freund TF, Katona I, Sensi SL, et al. Brain monoglyceride lipase participating in endocannabinoid inactivation. *Proc Natl Acad Sci U S A* 2002;99:10819–10824.
- [5] Zechner R, Zimmermann R, Eichmann TO, Kohlwein SD, Haemmerle G, Lass A, et al. FAT SIGNALS – lipases and lipolysis in lipid metabolism and signaling. *Cell Metab* 2012;15:279–291.
- [6] **Nomura DK, Morrison BE**, Blankman JL, Long JZ, Kinsey SG, Marcondes MC, et al. Endocannabinoid hydrolysis generates brain prostaglandins that promote neuroinflammation. *Science* 2011;334:809–813.
- [7] Mallat A, Teixeira-Clerc F, Lotersztajn S. Cannabinoid signaling and liver therapeutics. *J Hepatol* 2013;59:891–896.
- [8] **Habib A, Chokr D**, Wan J, Hegde P, Mabire M, Siebert M, et al. Inhibition of monoacylglycerol lipase, an anti-inflammatory and antifibrogenic strategy in the liver. *Gut* 2019;68:522–532.
- [9] Zerrad-Saadi A, Lambert-Blot M, Mitchell C, Bretes H, Collin de l'Hortet A, Baud V, et al. GH receptor plays a major role in liver regeneration through the control of EGFR and ERK1/2 activation. *Endocrinology* 2011;152:2731–2741.
- [10] Macal M, Jo Y, Dallari S, Chang AY, Dai J, Swaminathan S, et al. Self-renewal and Toll-like receptor signaling sustain exhausted plasmacytoid dendritic cells during chronic viral infection. *Immunity* 2018;48:730–744.e735.
- [11] Dobin A, Davis CA, Schlesinger F, Drenkow J, Zaleski C, Jha S, et al. STAR: ultrafast universal RNA-seq aligner. *Bioinformatics* 2013;29:15–21.
- [12] Traore M, Gentil C, Benedetto C, Hogrel JY, De la Grange P, Cadot B, et al. An embryonic CaV β 1 isoform promotes muscle mass maintenance via GDF5 signaling in adult mouse. *Sci Transl Med* 2019;11:eaaw1131.
- [13] Gacem N, Kavou A, Zerad L, Richard L, Mathis S, Kapur RP, et al. ADAR1 mediated regulation of neural crest derived melanocytes and Schwann cell development. *Nat Commun* 2020;11:198.
- [14] Chiot A, Zaïdi S, Iltis C, Ribon M, Berriat F, Schiaffino L, et al. Modifying macrophages at the periphery has the capacity to change microglial reactivity and to extend ALS survival. *Nat Neurosci* 2020;23:1339–1351.
- [15] Naro C, Jolly A, Di Persio S, Bielli P, Setterblad N, Alberdi AJ, et al. An orchestrated intron retention program in meiosis controls timely usage of transcripts during germ cell differentiation. *Dev Cell* 2017;41:82–93.e84.
- [16] Love MI, Huber W, Anders S. Moderated estimation of fold change and dispersion for RNA-seq data with DESeq2. *Genome Biol* 2014;15:550.
- [17] Liao Y, Wang J, Jaehnig EJ, Shi Z, Zhang B. WebGestalt 2019: gene set analysis toolkit with revamped UIs and APIs. *Nucleic Acids Res* 2019;47:W199–W205.
- [18] Minamino T, Ito Y, Ohkubo H, Hosono K, Suzuki T, Sato T, et al. Thromboxane A₂ receptor signaling promotes liver tissue repair after toxic injury through the enhancement of macrophage recruitment. *Toxicol Appl Pharmacol* 2012;259:104–114.
- [19] Miura Y, Fukui N. Prostaglandins as possible triggers for liver regeneration after partial hepatectomy. A review. *Cell Mol Biol Incl Cyto Enzymol* 1979;25:179–184.
- [20] De Luján Alvarez ML, Lorenzetti F. Role of eicosanoids in liver repair, regeneration and cancer. *Biochem Pharmacol* 2021;192:114732.
- [21] Minamino T, Ito Y, Ohkubo H, Shimizu Y, Kojo K, Nishizawa N, et al. Adhesion of platelets through thromboxane A₂ receptor signaling facilitates liver repair during acute chemical-induced hepatotoxicity. *Life Sci* 2015;132:85–92.
- [22] Yang Z, Zhang J, Wang Y, Lu J, Sun Q. Caveolin-1 deficiency protects mice against carbon tetrachloride-induced acute liver injury through regulating polarization of hepatic macrophages. *Front Immunol* 2021;12:713808.
- [23] Cordero-Espinoza L, Huch M. The balancing act of the liver: tissue regeneration versus fibrosis. *J Clin Invest* 2018;128:85–96.
- [24] Campana L, Esser H, Huch M, Forbes S. Liver regeneration and inflammation: from fundamental science to clinical applications. *Nat Rev Mol Cell Biol* 2021;22:608–624.
- [25] Gilgenkrantz H, Mallat A, Moreau R, Lotersztajn S. Targeting cell-intrinsic metabolism for antifibrotic therapy. *J Hepatol* 2021;74:1442–1454.
- [26] **Teixeira-Clerc F, Belot MP, Manin S**, Deveaux V, Cadoudal T, Chobert MN, et al. Beneficial paracrine effects of cannabinoid receptor 2 on liver injury and regeneration. *Hepatology* 2010;52:1046–1059.
- [27] **Mukhopadhyay B, Cinar R**, Yin S, Liu J, Tam J, Godlewski G, et al. Hyperactivation of anandamide synthesis and regulation of cell-cycle progression via cannabinoid type 1 (CB1) receptors in the regenerating liver. *Proc Natl Acad Sci USA* 2011;108:6323–6328.
- [28] Wernze H, Tittor W, Goerig M. Release of prostanoids into the portal and hepatic vein in patients with chronic liver disease. *Hepatology* 1986;6:911–916.
- [29] Rudnick DA, Perlmutter DH, Muglia LJ. Prostaglandins are required for CREB activation and cellular proliferation during liver regeneration. *Proc Natl Acad Sci USA* 2001;98:8885–8890.
- [30] Tsujii H, Okamoto Y, Kikuchi E, Matsumoto M, Nakano H. Prostaglandin E₂ and rat liver regeneration. *Gastroenterology* 1993;105:495–499.
- [31] Nissim S, Sherwood RI, Wucherpennig J, Saunders D, Harris JM, Esain V, et al. Prostaglandin E₂ regulates liver versus pancreas cell-fate decisions and endodermal outgrowth. *Dev Cell* 2014;28:423–437.
- [32] **Zhang Y, Desai A**, Yang SY, Bae KB, Antczak MI, Fink SP, et al. Inhibition of the prostaglandin-degrading enzyme 15-PGDH potentiates tissue regeneration. *Science* 2015;348:aaa2340.
- [33] Nishiguchi S, Otani S, Matsui-Yuasa I, Morisawa S, Monna T, Kuroki T, et al. Inhibition by interferon ($\alpha + \beta$) of mouse liver regeneration and its reversal by putrescine. *FEBS Lett* 1986;205:61–65.
- [34] Radaeva S, Jaruga B, Hong F, Kim WH, Fan S, Cai H, et al. Interferon-alpha activates multiple STAT signals and down-regulates c-Met in primary human hepatocytes. *Gastroenterology* 2002;122:1020–1034.
- [35] Coulombe F, Jaworska J, Verway M, Tzelepis F, Massoud A, Gillard J, et al. Targeted prostaglandin E₂ inhibition enhances antiviral immunity through induction of type I interferon and apoptosis in macrophages. *Immunity* 2014;40:554–568.